Laser & Photon. Rev. **1**, No. 4, 334–348 (2007) / **DOI** 10.1002/lpor.200710021

Abstract One of the great challenges in photonics has been to modify silicon to enhance light emission properties. In this review article we survey recent studies which have generated light from silicon in a variety of ways including introduction of emissive centers, anodization, fabrication of quantum-confined structures and by utilizing non-linear effects. Each method offers insight into silicon as an emissive medium, but no one method has proven effective enough a light source to compete with established technologies based on III-V and II-VI compound semiconductors, and in particular no one method of inducing light emission in silicon has made possible an electrically-pumped silicon laser.

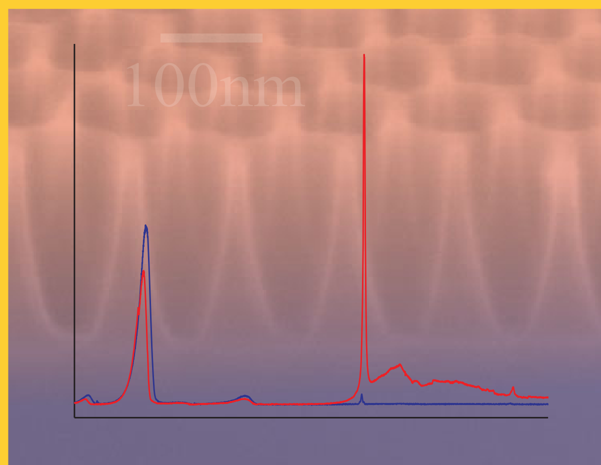

Photoluminescence spectra from nanopatterned silicon superimposed on a scanning electron micrograph of the emissive structure.

© 2007 by WILEY-VCH Verlag GmbH & Co. KGaA, Weinheim

Silicon as an emissive optical medium

Jeffrey M. Shainline [1] *and Jimmy Xu* [1,2,*]

[1] Department of Physics, Brown University
[2] Division of Engineering, Brown University

Received: 17 September 2007, Revised: 02 October 2007, Accepted: 17 October 2007
Published online: 13 November 2007

Key words: silicon; photonics; silicon laser; photoluminescence; electroluminescence

PACS: 61.72.J-, 41.20.-q, 42.60.By, 61.46.-w, 78.20.Ek, 78.45.+h, 78.55.-m, 78.60.Fi

1. The challenge of extracting light from Si

The effort to devise structures of silicon (Si) which efficiently and controllably emit light is a modern instance of the archetypal human-versus-nature conflict. The effort is driven by a natural desire: to integrate novel optical circuitry into well-established electronic designs to make possible new information processing and storage architectures. Since the overwhelming majority of existing electronics is manifest in Si, it seems intuitive that one elegant approach would be to integrate Si-based photonic devices into the Si-based electronic devices. Nature presents a quandary: the extremum of the conduction band at the Brillouin zone center is a maximum in Si; six symmetric Δ valleys lie in the X directions 1.1 eV above the top of the valence band at room temperature. Electron-hole recombination therefore requires a phonon. In bulk Si, the cross section for this three-body process is small, so this, the dominant luminescence pathway in pristine, bulk Si, is very inefficient. Recombination is almost entirely via non-radiative pathways at room temperature. However, at low temperature the non-radiative processes are suppressed along with phonon population and a large variety of radiative recombination pathways become observable; low-temperature photoluminescence is one way to gain insight into the physics of electron-hole radiative recombination in Si. A low-temperature photoluminescence spectrum of bulk Si is shown in Fig. 1.

The story of luminescence from Si is a story of looking at the same medium from new angles, placing it in different environments, and stimulating it with strategic perturbations. A central challenge has been that modifica-

Corresponding author: e-mail: Jimmy_Xu@Brown.edu

© 2007 by WILEY-VCH Verlag GmbH & Co. KGaA, Weinheim

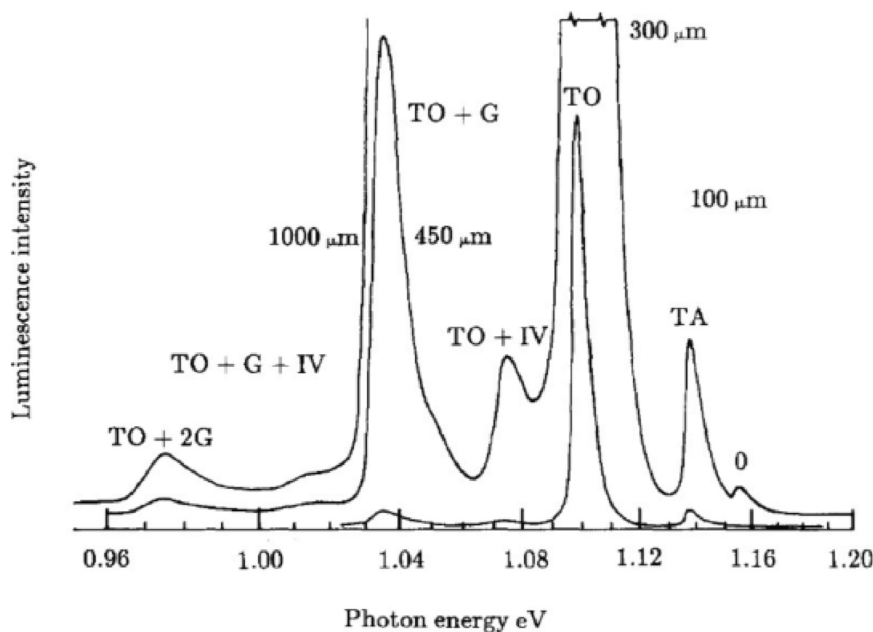

Figure 1 Si photoluminescence taken from the 1989 review of emissive point defects in Si written by Gordon Davies and cited in [1]. The spectra are taken at 26 K and recorded with four different slit widths (1000 µm, 450 µm, 300 µm and 100 µm) to give varying amplification and resolution. The labels refer to the combinations of phonons which are involved in the various luminescence pathways. G is the $k = 0$ optical mode. The peak labeled 0 is the ideally-forbidden zero-phonon component.

tions intended to augment radiative capability necessarily change the structure and in so doing introduce new nonradiative mechanisms and additional optical losses. So, as in many tales of active photonics, gain is the protagonist in conflict with loss. In this review article we analyze the photonic properties of Si [2–5], but not how Si structures can guide or modulate light [5]; our attention is kept on Si as an emissive medium [4, 6, 7]. Our aim is to identify the variety of techniques by which light has been drawn from Si, to outline the web of thinking which connects these techniques, and to distill the common wisdom which has been acquired through the study of Si in its myriad forms. As in any story of humans against nature, the only means by which humans can progress is to acquire a deep understanding of the nature in which we abide. Our understanding of Si is still evolving.

The indirect bandgap of Si is an important element of the context in which the science of Si photonics exists. The overwhelming success of CMOS technologies based on Si is another important element of the context [8]. When the electronics revolution of the 20th century became intertwined with crystalline Si, enormous research efforts became dedicated to exploring the structural and electronic properties of Si. The performance of electronic devices depends crucially on the quality of the Si lattice, and predictions regarding how devices will respond to perturbations such as dopants, strain, dislocations, surfaces etc., requires knowledge not just of a pristine Si lattice, but also of how the material behaves when it departs in any way from the form we know well – that of an ideal, infinite crystal.

We proceed now to discuss the luminescence which results from a variety of types of modifications to pristine Si. In particular, we discuss the luminescence from point defects, erbium-doped Si, porous Si, quantum confined structures including superlattices, quantum wires and nanocrystals; we discuss the effects of strain on the optical properties of Si and the luminescence by extended defects such as $\{311\}$ defects and dislocation loops which are large enough to introduce a sizeable strain perturbation to the lattice. In addition to the discussion of these techniques which generate light from Si by modifying the Si in various ways, we also discuss Raman scattering and other non-linear methods for obtaining light at one wavelength by down conversion of light pumped in at a higher energy. We attempt to highlight the key advantages and drawbacks of each method of utilizing Si as a light-emitting medium, to draw parallels between different methods where they are valid, and to emphasize the lessons which have been learned which offer insight into how to produce high-gain structures without incurring devastating loss.

2. Point defects

A pristine, crystalline lattice is an idealization. Even the highest-quality crystalline structures realizable to date contain many lattice vacancies and substitutional or interstitial impurities. Any such localized departure from the crystalline order is referred to as a point defect; point defects are usually comprised of one or a few vacancies or impurities interacting with the lattice. Such defects are always present after the growth of a crystal, and more are introduced in the steps necessary to process semiconductor devices. Solid state scientists beginning in the 1950s and continuing through the present day have explored the nature of a multitude of species of point defects in Si [1, 11–16]. They have been most commonly produced via ion, gamma ray, neutron or electron irradiation. An especially comprehensive review of optically-active point defects in Si is contained in [1].

Several effective techniques for studying defects in Si leverage the interaction of Si and of the defects with the

© 2007 by WILEY-VCH Verlag GmbH & Co. KGaA, Weinheim

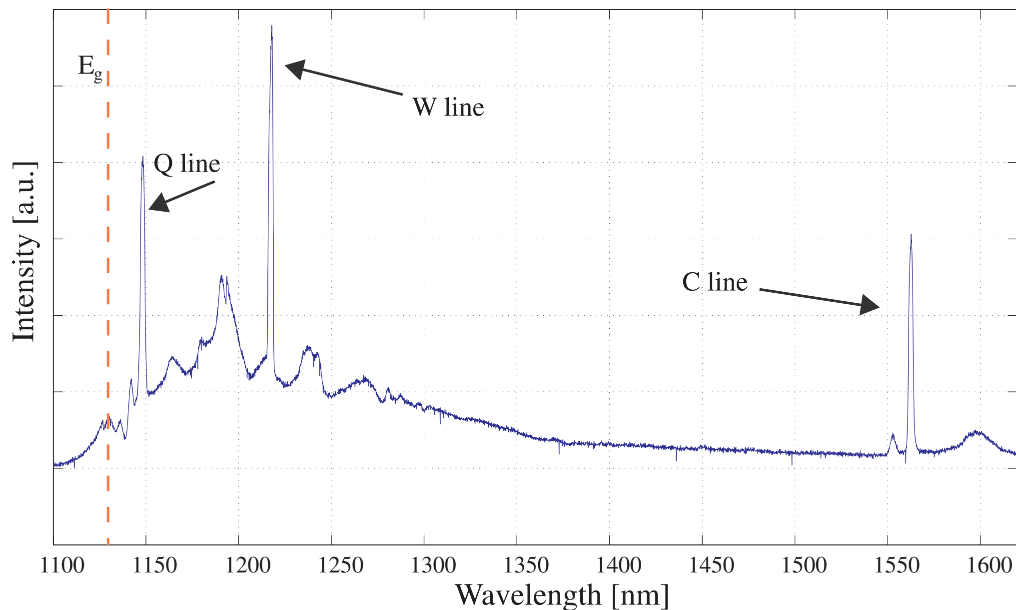

Figure 2 PL spectrum of Si bombarded with 100 keV Si^+ to a fluency of $10^{14}Si^+/cm^2$ and annealed at 250℃ for 30 min. The ZPL at 1218 nm dominates the spectrum. It is the well-known *W* line to be discussed later in the present article. The ZPL at 1149 nm is believed to be the *Q* line associated with a C-Li complex [9]. There is believed to be a forbidden transition at the same center observable below 2 K. The Li and C present in the lattice are residual contaminants introduced during the growth of the crystal. The broader luminescence from 1149 nm beyond 1218 nm are from a variety of phonon replicas of the *Q* center and the *W* center as well as a multitude of other weakly-luminescing centers. The ZPL at 1560 nm is the *C* line, believed to be associated with a C-O complex [10]. The band edge luminescence is observable at 1130 nm. However, the presence of so much damage in the lattice and so many optically active defects makes band-edge radiative recombination unlikely.

electromagnetic field. The aim in early research was to utilize techniques such as photoluminescence (PL), optical absorption, cathodoluminescence and electroluminescence, photothermal ionisation, and two-beam absorption [1], as well as electron paramagnetic resonance and deep-level transient capacitance spectroscopy [17] to understand the nature of point defects so they could be removed or minimized. In recent years some of these studies have reoriented their mission and have become dedicated to understanding the nature of certain point defects so their optical properties can be maximally utilized. Consideration of point defects for lasing is given in [18].

Point defects give rise to states in the band gap. The vast majority of point defects are not optically active and simply serve as non-radiative recombination pathways. Some point defects, however, give rise to pairs of states in the band gap with a non-vanishing electric dipole matrix element. PL spectra of samples with these optically-active point defects are characterized by narrow lines, called zero-phonon lines (ZPLs). An example of such a PL spectrum is shown in Fig. 2. A point defect with two electric-dipole-connected states (E_1 and E_2) in the band gap gives rise to a four level system. The conduction band edge is the highest energy level, and transition from E_c to E_2 is in general a fast, phonon-assisted process. The transition from E_2 to E_1 is the optical transition. Non-radiative transition from E_1 to E_v is also fast. Therefore, obtaining population inversion with E_2 over E_1 seems like a sensible goal. However, it is often the case that effects such as exciton thermalization before and after trapping, transitions from E_2 to E_c and non-radiative recombination from E_c to E_v quench the luminescence above a defect-dependent temperature which is always quite low and is usually below liquid N_2 temperature.

In this article we focus our emissive defect discussion on two point defects in particular which have played a role in recent advances. They are the carbon-related *G* center and the *W* center, which is believed to be composed of three Si self-interstitials. While our attention is focused on two specific point defects, many of the concepts relevant to these two optically emissive complexes can be applied to other optically emissive point defects in the Si lattice.

A *G* center [17, 19, 20] is a point defect comprised of two carbon atoms and one Si interstitial atom [17]. The nature of the *G* center is complicated by the fact that it can exist in two atomic configurations; these two configurations are referred to in the literature as the A and B configuration. In the A configuration a carbon atom substitutes a Si atom at one lattice site and an adjacent lattice site is shared by a second carbon atom and a Si atom. In the B configuration the two adjacent lattice sites are both occupied by carbon atoms and the Si interstitial is positioned between the two carbon atoms. These configurations are

© 2007 by WILEY-VCH Verlag GmbH & Co. KGaA, Weinheim

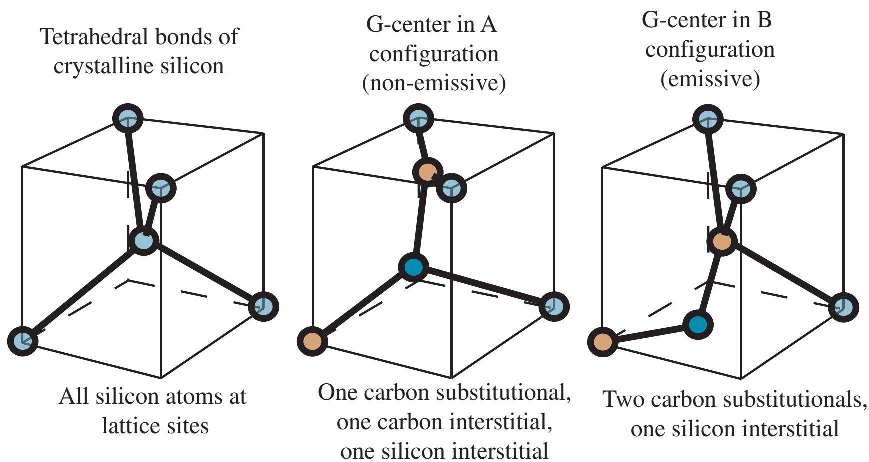

Figure 3 Schematic of the *G* center. a) Tetrahedral structure of Si bonds. b) *G* center in the non-emissive A configuration. c) *G* center in the emissive B configuration. Atoms involved in the *G* center are depicted in full opacity whereas atoms not participating in the point defect are shown as semitransparent.

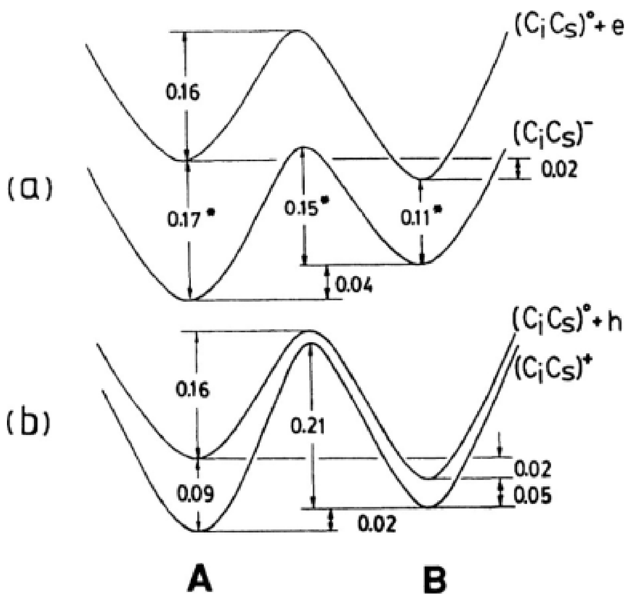

Figure 4 Configurational-coordinate energy diagram for the *G* center. The units are eV. (a) The defect acceptor state. (b) The defect donor state. The A and B at the bottom refer to the A and B configuration of the bistable *G* center. This figure is from [17].

illustrated in Fig. 3. The configurational-coordinate for the *G* center is shown in Fig. 4.

Substitutional carbon atoms are necessary for *G* center formation and occur naturally in Si wafers at concentrations between 10^{15} and 10^{17} atoms/cm^3 depending on the crystal growth technique [1]. A *G* center is created when a mobile interstitial carbon atom (C_i) binds with a substitutional carbon atom (C_s). It is hypothesized that Si interstitials (Si_i) are present from growth or created in a damage event. A mobile Si_i can migrate at room temperature to a lattice site occupied by a C_s. The C_s then gives its lattice site to the Si_i via the Watkins exchange mechanism [21]. The resulting mobile C_i can then migrate until it binds to a C_s forming a $\mathrm{C}_s\mathrm{C}_i$ pair, known as the *G* center. *G*-center creation depends both on the density of C_s present in the lattice [22] and on the density of introduced Si_is. It should be pointed out that many other C-related and Si_i-related centers exist, and treatments which give rise to the *G* center (or any one particular center) are likely to give rise to a multitude of competing radiative and non-radiative defect complexes.

The optical properties of the *G* center are intimately connected to the atomic configuration of the *G* center. The *G* center is bistable and can alternate between the A and B configurations. The mechanism of luminescence in Si containing *G* centers depends on the position of the Fermi level. The mechanism of luminescence in *p*-type material is shown schematically in Fig. 5. Both the A and B configurations can trap an electron from the conduction band in an "acceptor state" or trap a hole from the valence band in a "donor state". Note here the terms acceptor and donor are taken from the point of view of the defect. Only the B configuration of the *G* center is optically active. Excitation is the result of a sequential capture of an electron and a hole by the *G* center. The *G* line at 1278 nm is the result of an electric-dipole-mediated transition between two states of the G center in the B configuration.

Recent work utilized the optical activity of *G* centers to achieve stimulated emission in nanopatterned silicon-on-insulator (SOI) [23]. In the study by Cloutier et al., *G* centers became the emitter somewhat by accident. The original intention of the study was to explore the effects of local manipulation of the Si lattice. Because the optical properties of a crystal are dictated by the atomic nature of the lattice, many efforts in photonics modify the atomic configuration of a material by means such as irradiation, anodization, fabrication of quantum confined structures, etc. In the work by Cloutier et al., an SOI wafer was patterned using reactive ion etching (RIE) to contain an array of nanopores, as shown in Fig. 6. The intention was to investigate the effects of such a controllable, nanoscale manipulation on the optical properties. The *G* line was ob-

 © 2007 by WILEY-VCH Verlag GmbH & Co. KGaA, Weinheim

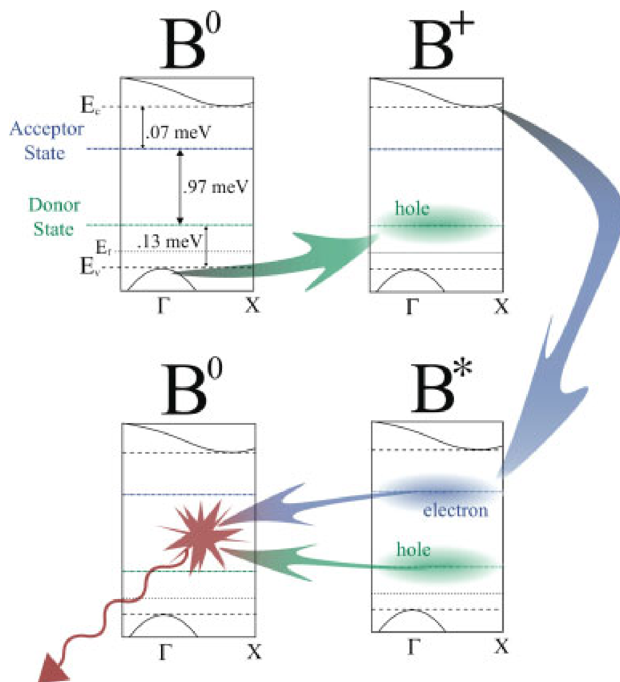

Figure 5 Schematic of the luminescence mechanism in *p*-type Si.

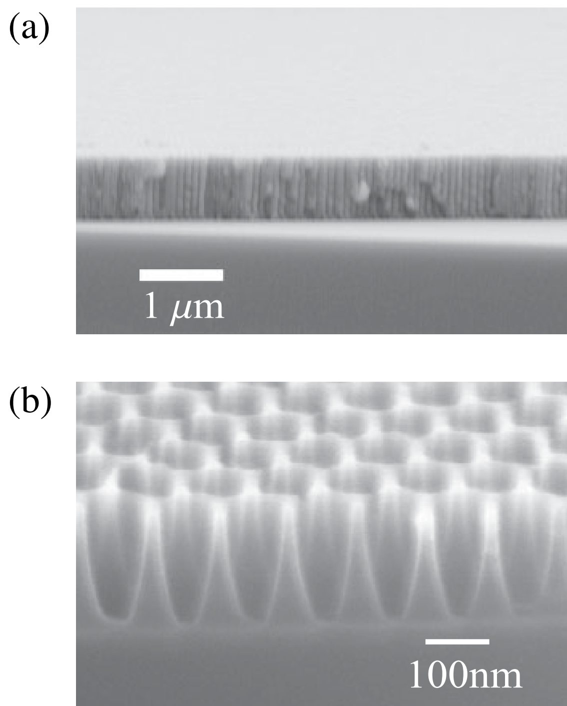

Figure 6 (a) An anodozided aluminum oxide membrane is placed atop an SOI wafer and used as an etch mask for RIE as described in [23]. (b) The structure after RIE and AAO removal. This sample was studied in [24].

served in the resulting structure and quickly became the focus of the study. In fact, the line at 1,278 nm in nanopatterned Si was originally thought to be due to the A center – an oxygen-vacancy complex – because early research in the field attributed the luminescence at 1,278 nm to the A center [11]. The A center and the *G* center were confused because of their similar deep-level transient capacitance spectroscopy signals. The hypothesis was later formed that interstitials created in the RIE process combine with C_s present in the lattice from the growth phase to form *G* centers in the process described above. Evidence that lasing occurred in the structure is presented in [23], and PL from the sample is shown in Fig. 7. The major advantage this method of *G* center introduction has over introduction via ion, gamma ray, or electron bombardment is that the damage to the lattice from RIE is contained in thin layers at the pore walls, leaving the remainder of the crystal pristine and capable of providing and preserving the photo carriers and funneling them to the emissive *G* centers in the pore side walls while incurring little additional optical loss.

A subsequent study [24] demonstrated the significance of the concentration of substitutional carbon in the lattice prior to nanopatterning. In [24] a carbon-rich lattice was obtained by amorphizing the Si lattice by bombardment with $10^{15}\ \mathrm{Si^+ cm^{-2}}$. This was followed by implantation of $10^{14}\ \mathrm{C^+ cm^{-2}}$, and rapid thermal annealing (RTA) in order to take advantage of the increased solid solubility of C in Si at the interface between crystalline and amorphous Si. This technique increased the luminescence from *G* centers by a factor of 30, as shown in Fig. 8. PL studies indicated that the annealing was sufficient to return the lattice to a state of high-quality crystal after the amorphization and carbon implantation. However, the procedure necessarily creates a more damaged lattice than was present before the treatment.

Because so many attempts have been made to get laser emission from the band edge, it may seem intuitive that any emission line less intense than the band edge PL is not likely to lase. This study indicates that it is possible to engineer defect creation to increase the peak intensity of a ZPL above the peak of the band edge PL without decreasing the band edge PL. But a word of caution is also in order. The intensity of light should not be the criterion by which we gauge whether or not a medium could permit lasing. One must keep in mind the amount of loss relative to the amount of gain in a cavity cycle. When designing systems to operate at room temperature, one must keep in mind that band-edge luminescence can be reabsorbed throughout the structure, but one tactic that has proven useful in several photonic devices is to keep the emissive region spatially localized and energetically below the band edge so most of the lasing mode is not in the region where reabsorption can occur.

While the work by Rotem et al. demonstrates progress in the use of point defects for optical activity in Si, progress toward overcoming another major challenge to point defect luminescence remains disappointing; all of the luminescence in nanopatterned *G*-center-based struc-

© 2007 by WILEY-VCH Verlag GmbH & Co. KGaA, Weinheim

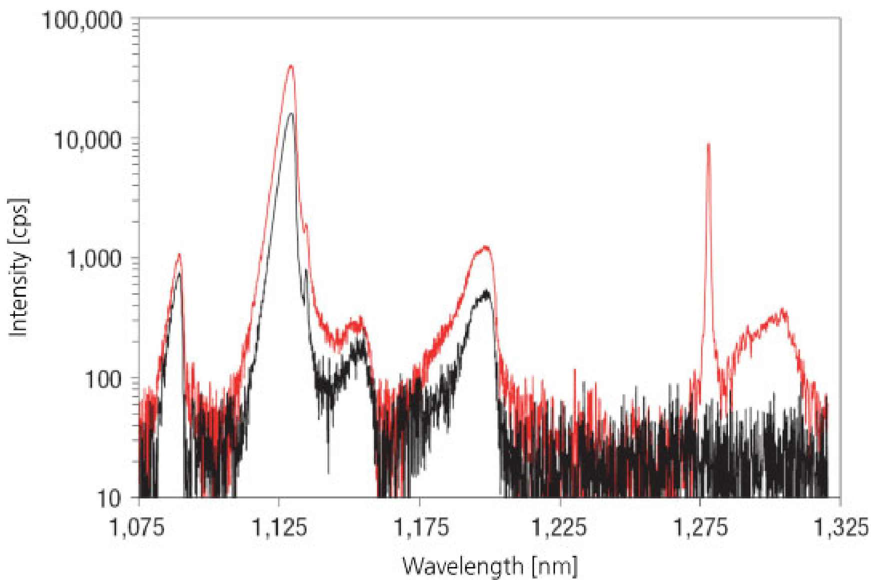

Figure 7 PL data taken from [23]. Spectra were acquired at 10 K. In black (lower spectrum) is the PL from an unpatterned SOI sample. The red (upper spectrum) is from the nanopatterned SOI sample. The 1,278 nm *G* line is present.

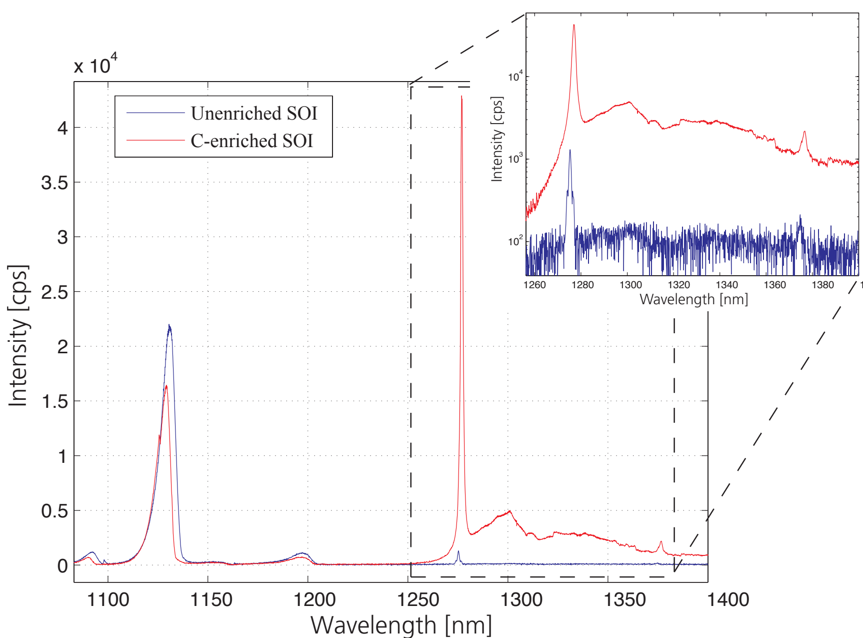

Figure 8 PL data taken from [24]. Spectra were acquired at 25 K. The blue (lower) spectrum shows data from nanopatterned SOI not prepared with a carbon-rich lattice. The C content in this lattice is the manufacturer specified concentration of $2.5 \times 10^{16} at./cm^3$. The red (upper spectrum) shows data from nanopatterned carbon-rich SOI. The C content in this lattice is approximately 10^{19}at.$/cm^3$. The *G* line from the nanopatterned carbon-rich SOI is 33 times more intense.

tures is quenched around 80 K. The real challenge will be to overcome this temperature limitation. Because this particular structure contains a great deal of surface area, this may be a setting in which surface passivation and its induced strain would be quite fruitful. To the knowledge of the authors, an attempt to passivate the surface of nanopatterned Si has not be undertaken.

W centers are believed to be trigonal complexes of three Si_is [25, 26]. The zero-phonon *W* line at 1218 nm is thought to occur from an electric-dipole-mediated transition between spin-singlet, non-degenerate orbital states at the *W* center [25]. This luminescence is quenched at even lower temperature than the *G* line. It is not observed above 40 K. *W* centers are appealing because they do not require the presence of a foreign atomic species in the lattice. *W* centers can be formed by irradiation of the lattice followed by annealing at 250℃. A common method for the introduction of *W* centers to the lattice is to bombard the lattice with Si^+ ions and then anneal. However, other methods of *W* center creation are possible as well [25].

In the recent work by Bao et al., a Si wafer was implanted with $^{28}Si^+$ to a fluency of $10^{15} cm^{-2}$ and with $^{34}S^+$ to a fluency of $10^{14} cm^{-2}$ at 77 K. These implantations amorphized the top 160 nm of the sample and were followed by an intense laser pulse from an $XeCl^+$ laser sufficient to melt the top 300 nm of the sample. The structure was then annealed at 275℃ for 2 minutes. Laser melting of the amorphous material allowed for recrystallization

© 2007 by WILEY-VCH Verlag GmbH & Co. KGaA, Weinheim

of Si supersaturated with S. This led to a heavily *n*-type region. It is believed that just beyond the laser-melted region is a layer of self-interstitial-rich material; it is in this region that *W* centers were formed during the RTA. Finally, electroluminescence at 1218 nm was demonstrated in this device. The estimated external quantum efficiency was 10^{-6}.

It is important to note that essentially the same mechanisms are at play in this study as in the nanopatterned *G* center study discussed above. In both, luminescence from ZPLs associated with point defects is utilized, and in both the relevant point defects are strategically produced in a local region of space in order to maintain higher-quality material elsewhere. Still, neither effort has moved the luminescence temperature higher. There will be more to say about this quandary later when we discuss utilizing a combination of techniques for increasing luminescence.

3. Erbium doping

Erbium (Er) doping of Si has been intensively studied for over twenty years, and early demonstrations of electroluminescence were very hopeful [27]. Er has an intra-4*f* shell transition with emission at 1.54 µm. This wavelength happens to fall at a minimum of silica absorption, a feature that is very appealing for telecommunications applications utilizing silica optical fibers. Er luminescence has much in common with the luminescence from point defects, but the nature of Er-doped Si differs enough from the nature of Si with optically-active point defects that it is appropriate to discuss it in an independent section. Most importantly, the nature of the optical transition of interest is defined by the electronic structure of Er, and is perturbed little by the presence of the Si lattice. This differs from the nature of point defects in that it is not meaningful to speak of the electronic structure of a point defect in the absence of the lattice; a point defect only exists within the atomic and electronic framework of the surrounding lattice. Still, Er-doped Si does not quite fall into the category of a system wherein Si is simply an inert host medium for the optical species. In Er-doped Si, Er (which, due to its rare-earth nature, ionizes to Er^{3+}) maintains key properties of its electronic structure, but is also intimately connected to the electronic band structure of the surrounding Si.

In the past fifteen years, a great deal has been learned about the behavior of Er in Si (see [28] and references cited therein). Er excitation in Si is similar to the excitation of many point defects in that it can occur through the sequential capture of electrons and holes at shallow levels in the gap, which may be, but are not necessarily, Er related. The energy is then transferred to the 4*f*-electron shell of the Er^{3+} ion [28, 29]. This excitation process is quite efficient at low-temperatures (10% excitation efficiency, cross section of $3 \times 10^{-15}\mathrm{cm}^2$, 7 orders of magnitude greater than direct photon absorption), and the luminescence is in a very narrow band resulting from the $^4I_{\frac{13}{2}} \rightarrow {}^4I_{\frac{15}{2}}$ atomic transition.

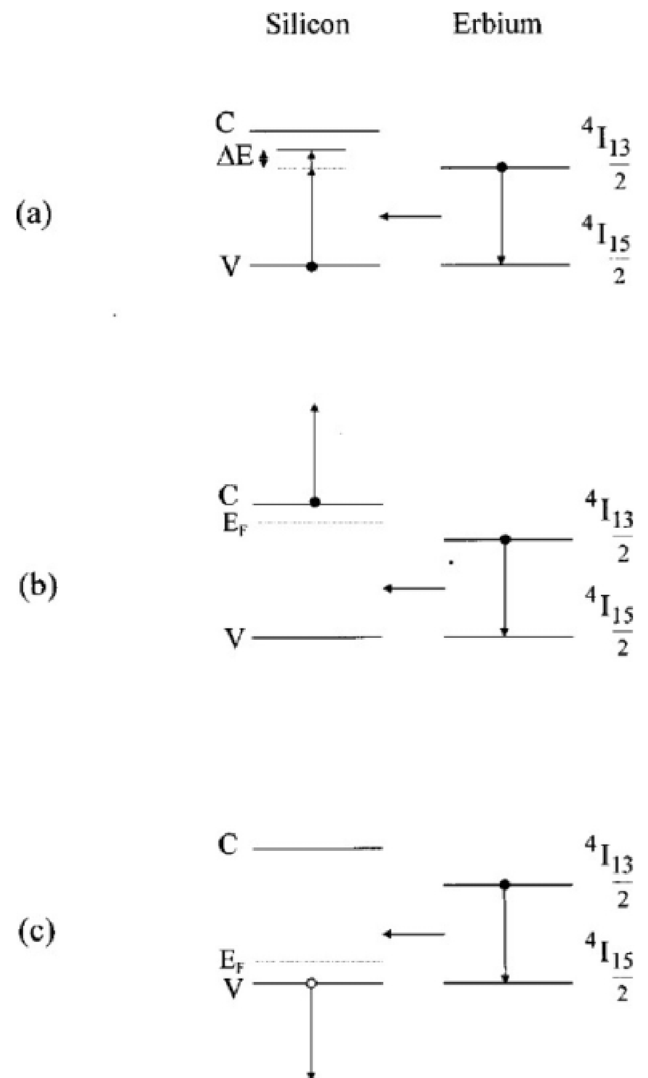

Figure 9 Schematic of potential deexcitation processes of Er^{3+} in Si. (a) The energy back transfer process wherein a captured electron is transferred back to the conduction band. The excited electron in the $^4I_{\frac{13}{2}}$ state transitions to the $^4I_{\frac{15}{2}}$ by promoting an electron from the valence band to another Er-related state in the band gap. The electron then thermalizes by transitioning to the conduction band, leaving the Er ion unpopulated. (b) The Auger process with free electrons and (c) with free holes [28].

Despite the many appeals of Er doping of Si, Er luminescence in Si suffers from the same weakness as point defects: the luminescence is quenched with temperature. An Auger process with either an electron or a hole are responsible for the quenching between 15 K and 120 K. Above 120 K an energy back transfer process makes luminescence improbable. The Auger processes and the back transfer process are illustrated in Fig. 9. This is a very similar scenario to the way in which luminescence from point defects is quenched with temperature. The fact that both mechanisms are so fundamental to the physical processes

© 2007 by WILEY-VCH Verlag GmbH & Co. KGaA, Weinheim

inherent in the systems makes them very hard to control or improve upon. Another obstacle is the quenching of emission due to the tendency of Er atoms to cluster together. This limits the concentration of Er incorporation in Si [30].

One method that has proven useful for extracting light from Er in a Si-based platform is to couple the Er ions to oxygen atoms [31] or Si nanocrystals or nanoclusters [32–34]. Optical gain [33] and electroluminescence [34] have recently been demonstrated in such devices. The cross section for excitation of Er ions by direct photon absorption is very small ($10^{-15}\mathrm{cm}^2$), but the absorption cross section of Si nanocrystals is much larger [35], and it has been shown in $\mathrm{SiO_2}$ films containing Si nanocrystals and Er^{3+} that the excitation of the Er is greatly enhanced by the presence of the nanocrystals [32]. It is believed the nanocrystals absorb the energy from the incident pump source and transfer it to the Er ions. In addition, deexcitation processes which occur in bulk Si are not a problem here, as the Er^{3+} ions are not embedded in a Si lattice.

One more scenario in recent work wherein Er has played the role of the emitter is in the demonstration of an Er-doped microdisk laser on a Si chip [36]. In this work high-Q silica microdisk cavities were fabricated on a Si chip and were doped with Er^{3+}. Threshold behavior was clearly demonstrated. While this work is not in the field of active Si photonics per se, it still represents a potential path forward for integrated optoelectronic circuit components.

4. Porous Si

The above discussion of point defects indicated how irradiation damage to the lattice can lead to optical activity. While point defects often result from irradiation damage, other processing techniques can also damage the lattice in a manner conducive to light generation. Anodization of Si in a hydrogen fluoride solution results in porous silicon (PS) which was found to give visible light emission at room temperature [37].

PS is a material wherein bulk Si has been etched into a mesh of nanoscale components. A sponge-like material results from the anodization of *p*-type Si, and a columnar structure with doping-dependent feature sizes results from the anodization of *n*-type Si. The emission from PS can be tuned by varying the etch recipe and is most commonly in the visible. Emission from PS is generally quite broad with a full width at half maximum of approximately 130 nm. The above-gap emission from PS suggests confinement of the electron and hole wave functions in the material is sufficient to increase the band gap. Further, the spacial confinement leads to broadening of electron amplitudes in momentum space, effectively allowing for phononless radiative transitions from the conduction to the valence band. This quantum confinement of electron and hole wavefunctions as well as of phonons is the mechanism which leads to increased radiative efficiency in Si nanocrystals and nanowires which will be discussed later. The narrow zero-phonon lines of point defects result essentially from transitions represented by a single matrix element of a pair of well defined states, but the broad luminescence from quantum-confined Si results from non-vanishing transition amplitudes between states distributed in the Brillouin zone.

Interpretation of PL spectra of PS has long been a subject of some contention. By analogy to other porous materials known to luminesce at above-bandgap wavelengths, it seems possible that the luminescence from PS could be due to an introduction of optically-active surface states. Attempts to model the luminescence as resulting from an array of nanowires of varying diameters has met with much success, but sceptics argue that any theory with as many parameters could fit such a curve. A recent letter [38] has proposed a parameter-free model in which consideration of the electron-hole interaction leads to prediction of excitonic gaps and optical absorption functions which are in good agreement with experimental data. This many-body treatment accurately predicts the optical properties of Si nanowires and porous Si and therefore may finally settle the nature of the luminescence from PS.

Although the discovery of efficient luminescence from PS was exciting, luminescence from PS is not without pitfalls. In particular distributing a limited amount of luminescence from PS over a broad band is not as desirable as narrow-band luminescence such as that resulting from transitions at point defects. Perhaps even more disconcerting is the manner in which the ability of a particular sample of PS to luminesce has a tendency to change in time.

To allow PS to emit in a narrow-band, PS microcavities, wherein a PS layer is sandwiched between two distributed PS Bragg reflectors has been utilized [39–41]. Using this technique, luminescence with a full width at half maximum of 14–20 nm in the wavelength range of 700–810 nm was achieved [41]. In this work by Xiong et al., the peak of the luminescence was able to be tuned over the range from 700–810 nm in steps of 5 nm by tuning the etching parameters, therefore the permittivity of the materials, and thus the wavelength of the dominant cavity mode.

The degradation in time of luminescence from PS is believed to be due to desorption of hydrogen molecules from the $\mathrm{Si}-\mathrm{H}_x$ bonds present at the PS surfaces after anodization. This desorption leaves dangling bonds which present non-radiative recombination pathways. To overcome this limitation many attempts at surface passivation have been made. Passivation of the surface with oxidation has been carried out [42], and nitridation of PS has also been executed and was shown to enhance the luminescence from PS and delay aging effects [43].

Although improvements to PS technology have been made which deal with some of the main drawbacks, PS as a platform for Si light emitting technologies has yet to be proven to be particularly valuable. Due to the harsh nature of the anodization process PS is in general a material with high electronic and optical losses. Thus, as we found in the case of creation of point defects via irradiation damage, we

© 2007 by WILEY-VCH Verlag GmbH & Co. KGaA, Weinheim

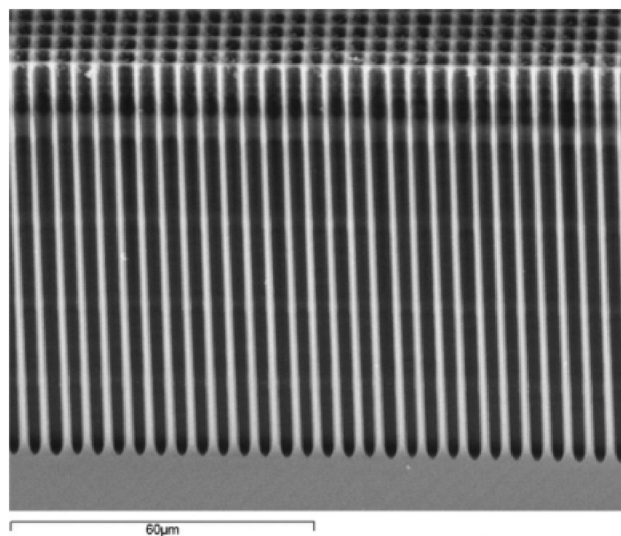

Figure 10 SEM image of a microporous Si photonic crystal. Electrochemical pore formation leads to a highly-uniform array of macropores with pore walls covered in a microporous PS structure. The microporous nature of the pore walls leads to quantum confinement effects and light emission [44].

find again that what we do to induce light emission in Si often damages the integrity of the material to the point where high performance operation of devices such as lasers has remained an elusive goal.

It should be mentioned that although PS is a low quality material with high electronic and optical losses, research in PS is still an active field indicating that progress is still being made. One recent study of macroporous Si [44] began the investigation of macroporous Si photonic crystals with luminescent microporous walls. The structure is shown in Fig. 10. Such attempts to couple emission to the engineered vacuum present a new way forward and may push PS beyond the existing boundaries.

5. Quantum confined structures

Quantum confined structures such as superlattices [45], nanowires [38,46], and nanocrystals [47–51] are structures with carrier confinement in one, two, and three spacial dimensions respectively wherein spacial confinement is the dominant mechanism for luminescence. Of these three geometries, nanocrystals have met with the most success as a Si-based light-emission platform. Si nanocrystals (Si-ncs) are commonly produced by thermal precipitation of Si atoms implanted in an SiO_2 matrix [49, 52], although chemical vapor deposition methods are also utilized [53]. A comprehensive account of the optical properties of Si-ncs is given in [48]

Having evolved from the concepts explored in the context of PS, Si-ncs have proven to be a source of light emission [49, 54] across most of the visible spectrum [55], and the wavelength of emission can be tuned by controlling the size of the formed Si-ncs [47]. In Si-based quantum confined structures confinement of carriers below the Si free-exciton Bohr radius of 5 nm is required to achieve carrier confinement effects. Enhanced luminescence from Si-ncs smaller than 5 nm is due to an increased overlap of electron and hole wave functions and a reduction in the rate of non-radiative events. Also, confinement of phonons [56] in configuration space leads to uncertainty in momentum space. This phonon k uncertainty leads to relaxation of the phonon k-selection rules [57] which govern radiative transition from the six symmetric Δ conduction band valleys to the Γ point of the valence band. This selection rule breaking also contributes to enhanced efficiency of luminescence in nanocrystals.

But whereas II-VI nanocrystals can have quantum yields as high as 80%-90%, luminescence from Si-ncs is much less efficient, usually with yields of a few percent. Such low efficiencies are believed to be due to non-radiative recombination at surface states. A recent study [50] found that with careful surface passivation quantum yields of approximately 60% could be achieved. This was done by avoiding oxygen during all stages of the Si-nc preparation. In this study Si-ncs were formed by plasma enhanced chemical vapor deposition and were maintained in a dry nitrogen atmosphere throughout the photoluminescence experiments. It was found that even temporary exposure to oxygen greatly decreased the luminescence from Si-ncs.

Another exciting development leveraging Si-ncs was the demonstration of field-effect electroluminescence from Si-ncs embedded in a thin oxide layer [52]. In this study, a 15 nm thick SiO_2 layer was implanted with $^{28}Si^+$ ions and annealed at 1,050℃ for 5 min to induce precipitation of Si-ncs. The structure used for electroluminescence and the mechanism for field-effect electroluminescence are shown in Fig. 11. In brief, a metal-oxide-semiconductor transistor structure supplies the carriers. The nanocrystal array is in the insulating SiO_2 layer. Electrons and holes are supplied sequentially via tunneling through the oxide to the nanocrystals to form excitons which then luminesce. Light is emitted through the semi-transparent gate. Unlike the operation of standard LEDs, there is no direct current flow.

Exciting progress has been made in understanding the physics of Si-nc light emission and in the development of technologies based on Si-ncs. But more creative thinking is need for an electrically-pumped Si-nc-based laser to be realized. It may be discovered that hybrid approaches with III-V or II-VI nanocrystals in Si cavities hold more promise for devices [58].

6. Strained Si

As the semiconductor industry waits patiently for a Si laser and attempts to squeeze slightly more efficiency from CMOS transistors with strain engineering, so too does the

© 2007 by WILEY-VCH Verlag GmbH & Co. KGaA, Weinheim

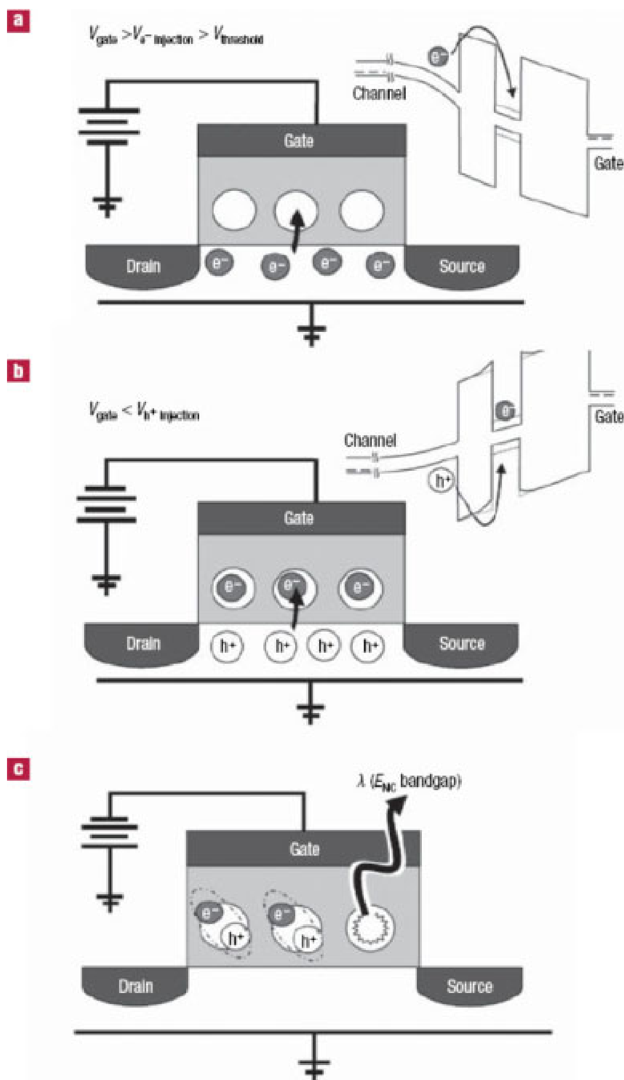

Figure 11 Schematic of the structure and sequential excitation process of field-effect electroluminescence of Si-ncs embedded in the oxide of a MOS structure. The inset band diagrams illustrate the relevant tunneling potentials. (a) Through Fowler-Nordheim tunneling, electrons populate the Si-ncs. (b) The Coulomb field of the negatively charged Si-ncs assists in the Fowler-Nordheim tunneling of holes to the nanocrystals. (c) The resulting excitons recombine radiatively.

personnel from Si photonics try to utilize strain to increase optical activity.

One method for utilizing strain to increase luminescence from Si leverages the zone folding which occurs in strained Si/Ge superlattices. In [59] photoluminescence from Si/Ge superlattices of varying thicknesses was studied. The strongest luminescence was found to originate from superlattices of ten monolayers with six monolayers Si and four monolayers Ge. In this structure tensile strain of 1% is believed to be present. This affects the band structure by breaking the sixfold-degenerated Δ conduction band minima into twofold-degenerate $\Delta_{\perp}$ minima in the direction perpendicular to the superlattice growth direction and fourfold-degenerate $\Delta_{||}$ in the superlattice planes. For a tensile strain of 1% the $\Delta_{\perp}$ are lower in energy than the $\Delta_{||}$ states. It is believed that Brillouin-zone folding effects lead to a quasidirect band gap with a dipole-allowed transition between the conduction and the valence bands. The luminescence found here was at 0.84 eV, a lower energy than the 1.1 eV band gap of bulk Si. This is evidence that the quasidirect gap resulting from the $\Delta_{\perp}$ minima is shifted to lower energy than the Δ minima of bulk Si.

Although this presents an interesting technique for enhancing Si light emission, the photoluminescence spectra in this study were taken at 5 K, and the optical activity does not persist to higher temperatures. In this situation it is likely that defects at the interfaces between the Si and Ge layers lead to non-radiative recombination.

A more recent study of 8 nm thick tensile strained SOI explored in detail the effects of strain on the low temperature photoluminescence from strained Si [60]. While this study was not focused on increasing the luminescence efficiency from Si it presents an interesting technique for quantifying the strain present in devices which leverage strain to enhance optical activity.

Much as defect scientists used PL to study defects and eventually engineered defects for the express purpose of creating PL, so too have researchers begun to engineer strain to give rise to more efficient luminescence. A Si LED operating at room temperature and leveraging the effects of strain has been demonstrated [61]. In this work a standard *p*-*n* junction operates as a conventional LED under forward bias. Because carrier diffusion to non-radiative recombination centers is the leading mechanism for loss in such an LED, strain is utilized to trap carriers in the junction region. Strain is incorporated in the device by introduction of dislocation loops. Dislocation loops are well studied [62] and are believed to be formed by the agglomeration of Si_is during annealing of radiation-damaged Si. In [61] the self-interstitials were created during the boron ion implantation necessary to create the *p*-*n* junction. Annealing for 20 minutes at 1,000℃ resulted in a dislocation loop array. It is believed that the strain from the dislocation loops creates a potential barrier, and that as carriers are injected across the junction this potential barrier traps carriers close to the junction region. Using this technique electroluminescence from the Si band edge at 1,160 nm is observed at room temperature. The output power of this device was approximately 20 µW, and the external quantum efficiency was 2×10^{-4}. Typical commercial GaAs LEDs have an external quantum efficiency of 10^{-2}.

7. {311} defects

The aforementioned LED which utilized dislocation loops to induce strain fields capable of trapping carriers in the depletion region is one example of utilizing extended defects to enhance optical activity. Other extended defects

© 2007 by WILEY-VCH Verlag GmbH & Co. KGaA, Weinheim

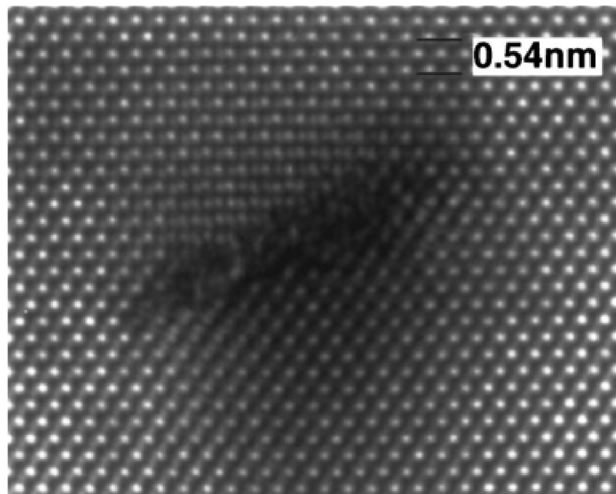

Figure 12 Transmission electron lattice image of a {311} defect with a width of 5 nm in a sample implanted with 10^{14} cm^2 Si ions and annealed at 750℃ [15].

with interesting optical properties are known, but few devices leverage these defects because, in general, Si with extended defects is a very high-loss material. Still, it is worth discussing briefly a particular extended defect known as the {311} defect. {311} defects have been studied in much detail [15, 62–65]. They are rod-shaped accumulations of Si_is in {311} planes of the Si lattice (see Fig. 12). These defects are optically active with narrow sub-bandgap emission at 903 meV at cryogenic temperatures. While emission from {311} defects is narrow at low temperatures, it is still broader than the ZPLs of point defects. What makes {311} defects worth mentioning is that their luminescence persists to higher temperatures; in particular, the luminescence from {311} defects was shown to decrease by only a factor of 30 from 4.2 to 240 K, as is shown in Fig. 13 from [15]. The persistence of the luminescence to higher temperature is due to exciton confinement in the strain field induced by the presence of the cluster of interstitials [15]. Most experimental studies of the optical properties of {311} defects have produced them by high doses of ions ($10^{12} - 10^{15}$ $Si^{+}cm^{-2}$) at MeV energies followed by annealing in the temperature range 680℃ to 800℃. Such a treatment is very damaging to the lattice, and it is unlikely that a high performance device could be achieved with this fabrication. However, if a more controlled introduction of {311} defects could be conceived, {311} defects may be a valuable source of luminescence from Si.

8. Raman conversion and other non-linear methods

Amidst the murky seas of Si photonics, one strategy has been to refrain from stirring the water in order to let

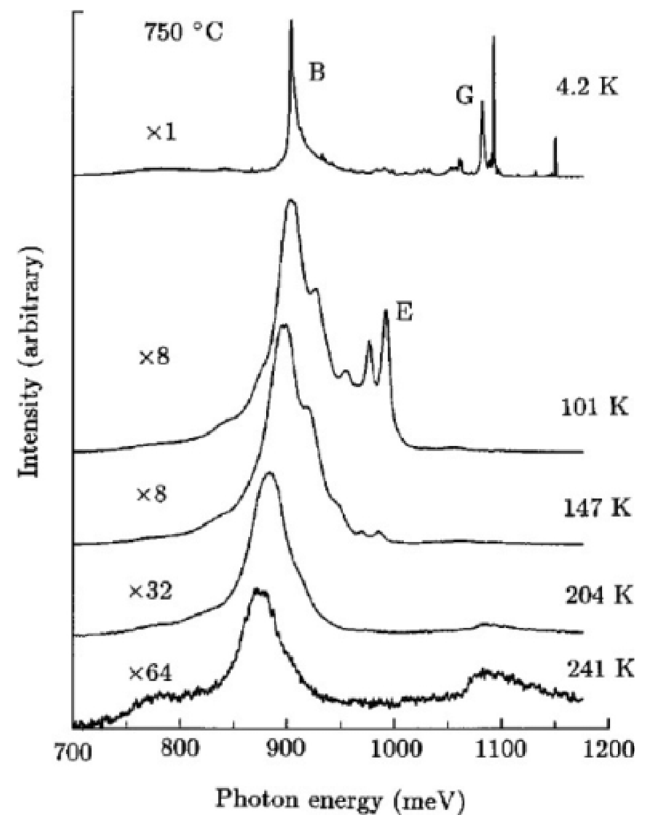

Figure 13 PL spectra at 4.2–240 K of samples implanted with $10^{14}cm^{-2}$ Si^{+} and then annealed at 750℃. Each spectrum has been multiplied by the factor shown. The feature labeled "B" is the luminescence due to {311} defects. Note that the ZPLs which were present at cryogenic temperature (the features marked "G", not to be confused with the *G* line) are completely quenched by 100 K. The band starting near 1,060 meV at 240 K is free-exciton emission. These data are taken from [15].

the waves and sediment calm; non-linear optical properties of pristine bulk Si allowed for the creation by Jalali and coworkers of a Raman conversion laser [66], the first demonstration of coherent light generation in Si. This was followed by work done at Intel which led to a continuous-wave laser [67]. These achievements generated great excitement in the field, and progress with Raman Si lasers continues. Recently a low-threshold continuous-wave Raman Si laser was demonstrated [68] (see Fig. 14). In this work a lasing threshold of 20 mW was achieved with slope efficiency of 28% and output power of 50 mW with a 25 volt reverse bias applied to the *p*-i-*n* Si wave guide. This reverse bias is applied to reduce the free carrier absorption in order to increase the efficiency of the non-linear conversion process. However, in the same work a device was fabricated with no reverse bias. In this case the lasing threshold was 26 mW with an output power of 10 mW. While Raman conversion has proven to be a successful method for obtaining light from Si [69–71] a few characteristics should be mentioned which distinguish it from the other

© 2007 by WILEY-VCH Verlag GmbH & Co. KGaA, Weinheim

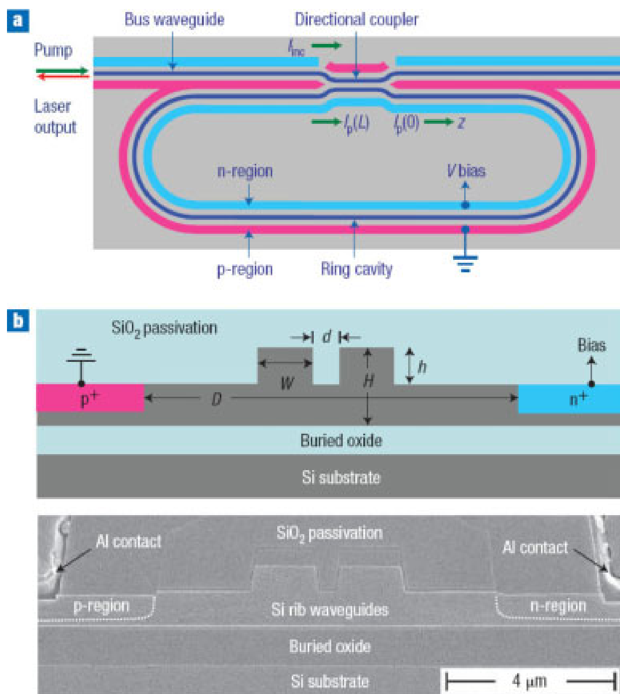

Figure 14 Configuration of the ring-cavity and waveguide cross-section of the structure utilized in [68] for the low-threshold Raman Si laser. (a) Schematic layout of the Si ring laser cavity with a p-i-n structure along the waveguides. (b) Schematic and SEM cross-section of the coupler region of a ring laser cavity.

methods of obtaining luminescence in Si. Due to the nature of Raman amplification a Raman laser will always necessitate an external optical pump. Therefore, a completely integrated electrically pumped Si laser based on Raman conversion is not a possibility. Additionally, the low efficiency of the $\chi^{(3)}$ process is a physical limitation with little room for improvement. This physical constraint requires cavity lengths on the order of centimeters to achieve sufficient gain. This is far too big to be practical for on-chip applications. Still, it should be noted that the progress in Si Raman photonics has been impressive and while the application of Raman Si lasers may not be for on-chip optoelectronic devices, other fields such as optical sensing and biomedical sciences may benefit from these technologies.

We also mention briefly that non-linear optical properties of Si have recently been used for active photonic devices in other ways. Four-wave mixing has recently been demonstrated in SOI waveguides [72]. In this study broadband optical parametric gain was demonstrated; net on/off gain over a wavelength range of 28 nm was achieved via phase-matched four-wave mixing. This is a third-order ($\chi^{(3)}$) process. Another recent study [73] induced a $\chi^{(2)}$ of approximately 15 pm V^{-1} by breaking the inversion symmetry by placing a straining layer atop a waveguide structure. This allowed for demonstration of an electro-optic modulator.

9. Synthesis of Techniques

There are many concepts laid out before us and many existing structures – each with strengths but none strong enough to stand alone. There are point defects with zero-phonon lines and a four-level structure but vanishing luminescence with increased temperature; Er doped Si with essentially the same strengths and weaknesses as point defects; porous Si with broader emission tuneable with anodization conditions, but a high-loss optical and electronic medium with a luminescence efficiency which decays in time; more controlled quantum-confined structures such as Si nanocrystals with potentially high-efficiency tunable luminescence and demonstrated electroluminescence, but still not competitive with III-V or II-VI nanocrystals, and emission in the visible, which is not advantageous for telecommunication applications; strain as a perturbation which can be conducive to optical activity, but which is not very helpful as a technique in isolation; extended defects which combine the benefits of optical activity with trapping due to strain, but which require damage to the lattice for creation; and Raman conversion, a third-order process which is inherently inefficient, requiring large cavities to obtain sizeable gain, and requiring an external optical pump.

These are the techniques of active Si photonics. The common threads of thinking are numerous and the barriers to electrically-pumped lasers are few but formidable. Perhaps what is required now is to draw upon several of these techniques to design structures which overcome the fundamental limitations by elegantly circumventing them. We know several facts:

1. The narrow-band luminescence from Er and point defects is appealing
2. This luminescence is quenched at room temperature due to the tendency of excited centers to release their trapped carriers to the conduction band
3. Strain effects, such as those present in dislocation loops and {311} defects, are capable of trapping excitons up to room temperature
4. Si nanocrystals have efficient optical absorption and emission at room temperature and are capable of transferring their energy to Er^{3+} and perhaps point defects as well

How can one merge these concepts into a blueprint for a laser? What structures come to mind? Hopefully many ideas come to many minds. One structure that is perhaps useful for illustrating how these concepts can play off each other is nanopatterned Si, as shown in Fig. 6. Raman peak broadening and shifts were observed in this structure [74, 75] and were taken as evidence that Si nanocrystals were formed in the nanopatterning process. The work in [23] and [24] clearly indicates that *G* centers are formed

© 2007 by WILEY-VCH Verlag GmbH & Co. KGaA, Weinheim

in the nanopatterning process. Are the nanocrystals coupled to the *G* centers? If so, how does this affect the luminescence? How can we accentuate the effect? If not, can we couple them? Further, the walls of the pores are riddled with defects [74]. It may be hypothesized that these defects give rise to a pseudocontinuum of states below the conduction band edge, making population of the *G* centers more likely. But does this also make thermal de-excitation of *G* centers more likely? And are these defect states really just providing non-radiative pathways for precious carriers? Can they be dealt with by surface passivation? Additionally, the surfaces of the pores are believed to be under strain [74], though exactly what type of strain is not clear. Does this strain help trap carriers in the G-center-rich regions near the pore walls? If so, why hasn't the luminescence temperature been increased? Also, how can we quantify this strain? It has not given rise to signatures in PL spectra, as in [60]. Can we enhance this strain effect until it is clearly playing a role in the luminescence?

Perhaps there are other directions we can go, even in the same nanopatterned Si platform. Suppose we were able to neatly fill the pores with a combination of nanocrystals and Er. The nanocrystals would efficiently pump the Er, as was shown in [32] or as in work on electroluminescence from Er-doped Si nanocluster-based devices [34]. Perhaps the hopping conduction of Si-ncs [76] could lead to excitation of nanocrystals to a depth unattainable by Fowler-Nordheim tunneling alone. Excited Er^{3+} would not loose its carriers to the conduction band at higher temperatures because it would not be coupled to the conduction band of the bulk crystal. Further, though previous studies have not taken advantage of this fact, nanopatterned Si is a two-dimensional triangular photonic crystal with finite extent in the third dimension. The pore spacing could be tuned to maximize the density of optical states at the emission wavelength, 1.54 µm. In such a structure, field-effect electroluminescence should be possible, as was demonstrated in a MOS structure in [52].

Or maybe platforms aside from nanopatterned Si hold more promise. Can we use the strain effects and optical properties of {311} defects but not introduce the defects in a way that is so damaging to the entire lattice? Can we introduce them locally, say, with a focused ion beam, and leave the lattice pristine elsewhere? Perhaps we only want the strain of {311} defects, but the optical activity of another species. Maybe we can locally introduce {311} defects or dislocation loops for their strain and an optically-active species of our choice so that the strain effects allow the optically-active center to be populated to room temperature.

10. Closing Remarks

We have discussed many of the techniques common today for generating light from Si. This review is not meant to be an exhaustive study, rather a sampling of some of the intriguing concepts emerging from a rich and exciting field of study.

As a final closing statement we note that while much of this article has focused on Si photonics for the purpose of creating on-chip optoelectronic devices, photonics in general is a burgeoning field with a great deal of fundamental physics still to be explored. For example, the recent work by Yang and John [77, 78] explores the quantum dynamics of excitons in a photonic-crystal – quantum-well heterostructure. Work by Vahala, Kimble and others explores cavity quantum electrodynamics in the context of ultrahigh-*Q* microresonators [79]. While many materials may be useful for these types of studies, it is likely that Si and SiO_2 will prove to be quite valuable. So, while utilizing Si as an active optical medium toward the end of on-chip, electrically-pumped Si lasers remains a priority, it is likely that scientists studying the fundamental physics of light in media will find active Si photonics a relevant field of study.

Acknowledgements We acknowledge the contributions from Efraim Rotem in the conceptualization of the physics of the G center, and ONR and AFOSR for the timely provision of funding support.

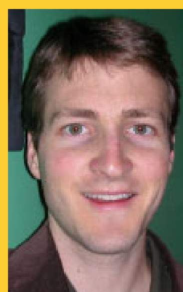

Jeffrey Shainline received a B.A. in physics from the University of Colorado, Boulder in 2005. He is currently a Ph.D. candidate in physics at Brown University. His interests include nanostructured photonic devices including periodic systems and sub-wavelength cavities for capturing, storing, guiding and generating light. A common theme in his work is the interplay between electronic and optical coupling in structures with metallic and dielectric components.

Jimmy Xu is the Charles C. Tillinghast Jr. '32 University Professor of Engineering and Physics at Brown University. Prior to coming to Brown in 1999, he was the James Ham Professor of Optoelectronics and Director of the Nortel Institute of Telecommunications at the University of Toronto. His current research interests are in atomic, molecular and quantum structures, phenomena, devices and sciences, sensors, emitters, lasers, and collective behaviors of large coupled quantum systems. Ongoing research includes silicon photonics, carbon nanotubes, nanoelectronic-molecule interfaces; arrayed quantum structures in metals, superconducting, molecules and semiconductors; DNA conductivity, DNA engineering; nano-electronic interfacing of redox proteins and cells.

© 2007 by WILEY-VCH Verlag GmbH & Co. KGaA, Weinheim

References

[1] G. Davies, Phys. Rep. **176**, 83–188 (1989).
[2] G. T. Reed and A. P. Knights, Silicon Photonics: An Introduction (Wiley, 2004).
[3] L. Pavesi and D. Lockwood, Silicon Photonics, Topics in Applied Physics, Vol. 94 (Springer Verlag, Heidelberg, 2004).
[4] B. Jalali and S. Fathpour, J. Lightwave Technol. **24**, 4600 (2006).
[5] M. Lipson, J. Lightwave Technol. **23**, 4222 (2005).
[6] S. S. Iyer and Y. H. Xie, Science **260**, 40 (1993).
[7] S. Ossicini, L. Pavesi, and F. Priolo, Light emitting silicon for microphotonics, Springer tracts in modern physics (Springer-Verlag, Berlin, Germany, 2003).
[8] N. Izhaky, M. T. Morse, S. Koehl, O. Cohen, D. Rubin, A. Barkai, G. Sarid, R. Cohen, and M. J. Paniccia, IEEE J. Sel. Top. Quantum Electron. **12**, 1688 (2006).
[9] E. Lightowlers, L. Canham, G. Davies, M. Thewalt, and S. Watkins, Phys. Rev. B **29**, 4517 (1984).
[10] K. Thonke, A. Hangleiter, J. Wagner, and R. Sauer, J. Phys. C **18**, L795 (1985).
[11] R.J. Spry and W.D. Compton, Phys. Rev. **175**, 1010 (1968).
[12] A. Bean, R. Newman, and R. Smith, J. Phys. Chem. Solids **31**, 739 (1970).
[13] C. E. Jones, E. S. Johnson, W. D. Compton, J. R. Noonan, and B. G. Streetman, J. Appl. Phys. **44**, 5402–5410 (1973).
[14] O. Awadelkarim, A. Henry, B. Monemar, J. Lindstrom, Y. Zhang, and J. Corbett, Phys. Rev. B **42**, 5635 (1990).
[15] D. Schmidt, B. Svensson, M. Seibt, C. Jagadish, and G. Davies, J. Appl. Phys. **88**, 2309 (2000).
[16] G. Davies, S. Hayama, L. Murin, R. Krause-Rehberg, V. Bondarenko, A. Sengupta, C. Davia, and A. Karpenko, Phys. Rev. B **73**, 165202 (2006).
[17] L. Song, X. Zhan, B. Benson, and G. Watkins, Phys. Rev. B **42**, 5765 (1990).
[18] A. Yukhnevich, Solid-State Electron. **51**, 489 (2007).
[19] G. Davies, H. Brian, E. Lightowlers, K. Barraclough, and M. Thomaz, Semicond. Sci. Technol. (UK) **4**, 200–206 (1989).
[20] A. Dolgolenko, M. Varentsov, and G. Gaidar, phys. stat. sol. (b) **241**, 2914–2922 (2004).
[21] G. W. Watkins, Phys. Rev. B **12**, 5824–5839 (1975).
[22] P. N. K. Deenapanray, N. E. Perret, D. J. Brink, F. D. Auret, and J. B. Malherbe, J. Appl. Phys. **83**, 4075–4080 (1998).
[23] S. Cloutier, P. Kossyrev, and J. Xu, Nature Mater. **4**, 887 (2005).
[24] E. Rotem, J. M. Shainline, and J. M. Xu, Appl. Phys. Lett. **91**, 051127 (2007).
[25] G. Davies, E. Lightowlers, and Z. Ciechanowska, J. Phys. C, Solid State Phys. (UK) **20**, 191 (1987).
[26] S. Hayama and G. Davies, J. Appl. Phys. **96**, 1754 (2004).
[27] H. Ennen, G. Pomrenke, A. Axmann, K. Eisele, W. Haydl, and J. Schneider, Appl. Phys. Lett. **46**, 381 (1985).
[28] F. Priolo, G. Franzo, S. Coffa, and A. Carnera, Phys. Rev. B **57**, 4443 (1998).
[29] T. Gregorkiewicz, D. T. X. Thao, J. M. Langer, H. H. P. T. Bekman, M. S. Bresler, J. Michel, and L. C. Kimerling, Phys. Rev. B **61**, 5369 (2000).
[30] A. Polman, G. van den Hoven, J. Custer, J. Shin, R. Serna, and P. Alkemade, J. Appl. Phys. **77**, 1256 (1995).
[31] R. Serna, J. Shin, M. Lohmeier, E. Vlieg, A. Polman, and P. Alkemade, J. Appl. Phys. **79**, 2658 (1996).
[32] M. Fujii, M. Yoshida, Y. Kanzawa, S. Hayashi, and K. Yamamoto, Appl. Phys. Lett. **71**, 1198 (1997).
[33] H. S. Han, S. young Seo, and J. H. Shin, Appl. Phys. Lett. **79**, 4568 (2001).
[34] F. Iacona, D. Pacifici, A. Irrera, M. Mirirtello, G. Franzo, F. Priolo, D. Sanfilippo, G. D. Stefano, and P. Fallica, Appl. Phys. Lett. **81**, 3242 (2002).
[35] D. Kovalev, J. Diener, H. Heckler, G. Polisski, N. Kunzner, and F. Koch, Phys. Rev. B **61**, 4485 (2000).
[36] T. J. Kippenberg, J. Kalkman, A. Polman, and K. J. Vahala, Phys. Rev. A **74**, 051802(R) (2006).
[37] L. Canham, Appl. Phys. Lett. **57**, 1046 (1990).
[38] M. Bruno, M. Palummo, A. Marini, R. D. Sol, and S. Ossicini, Phys. Rev. Lett. **98**, 036807 (2007).
[39] L. Pavesi, C. Mazzoleni, A. Tredicucci, and V. Pellegrini, Appl. Phys. Lett. **67**, 3280 (1995).
[40] L. Pavesi and P. Dubos, Semicond. Sci. Technol. (UK) **12**, 570 (1997).
[41] Z. H. Xiong, S. Yuan, Z. M. Jiang, J. Quin, C. W. Pei, L. S. Liao, X. M. Ding, X. Y. Hou, and X. Wang, J. Lumin. **80**, 137 (1999).
[42] H. Chen, X. Hou, L. Gubo, F. Zhang, S. Yuan, Y. Mingren, and X. Wang, J. Appl. Phys. **79**, 3282 (1996).
[43] A. Daami, G. Bremond, L. Stalmans, and J. Poortmans, J. Lumin. **80**, 169 (1999).
[44] S. Cheylen and T. Trifonov, A. Rodriguez, L. F. Marsal, J. Pallares, R. Alcubilla, and G. Badenes, Opt. Mater. **29**, 262 (2006).
[45] D. J. Lockwood, Z. H. Lu, and J. M. Baribeau, Phys. Rev. Lett. **76**, 539 (1996).
[46] S. Piscanec, M. Cantoro, A. Ferrari, J. Zapien, Y. Lifshitz, S. Lee, S. Hofmann, and J. Robertson, Phys. Rev. B **68**, 241312(R) (2003).
[47] T. Takagahara and K. Takeda, Phys. Rev. B **46**, 15578 (1992).
[48] D. Kovalev, H. Heckler, G. Polisski, and F. Koch, phys. stat. sol. (b) **215**, 871 (1999).
[49] L. Pavesi, L. D. Negro, C. Mazzoleni, G. Franzo, and F. Priolo, Nature **408**, 440 (2000).
[50] D. Jurbergs, E. Rogojina, L. Mangolini, and U. Kortshagen, Appl. Phys. Lett. **88**, 233116 (2006).
[51] F. Trani, D. Ninno, and G. Iadonisi, Phys. Rev. B **75**, 033312 (2007).
[52] R. J. Walters, G. I. Bourianoff, and H. A. Atwater, Nature Mater. **4**, 143–146 (2005).
[53] M. Cavarroc, M. Mikikian, G. Perrier, and L. Boufendi, Appl. Phys. Lett. **89**, 013107 (2006).
[54] H. Morisaki, F. Ping, H. Ono, and K. Yazawa, J. Appl. Phys. **70**, 1869 (1991).
[55] H. Takagi, H. Ogawa, Y. Yamazaki, A. Ishizaki, and T. Nakagiri, Appl. Phys. Lett. **56**, 2379 (1990).
[56] J. Zi, H. Buscher, C. Falter, W. Ludwig, K. Zhang, and X. Xie, Appl. Phys. Lett. **69**, 200 (1996).
[57] D. Kovalev, H. Heckler, M. Ben-Chorin, G. Polisski, M. Schwartzkopff, and F. Koch, Phys. Rev. Lett. **81**, 2803 (1998).

© 2007 by WILEY-VCH Verlag GmbH & Co. KGaA, Weinheim

[58] Z. Wu, Z. Mi, P. Bhattacharya, T. Zhu, and J. Xu, Appl. Phys. Lett. **90**, 171105 (2007).
[59] R. Zachai, K. Eberl, G. Abstreiter, E. Kasper, and H. Kibbel, Phys. Rev. Lett. **64**, 1055 (1990).
[60] J. Munguia, G. Bremond, J. D. L. Torre, and J. M. Bluet, Appl. Phys. Lett. **90**, 042110 (2007).
[61] W. L. Ng, M. A. Lourenco, R. M. Gwilliam, S. Ledain, G. Shao, and K. P. Homewood, Nature **410**, 192 (2001).
[62] S. Libertino, S. Coffa, and J. Benton, Phys. Rev. B **63**, 195206 (2001).
[63] J. Kim, F. Kirchoff, J. Wilkins, and F. Khan, Phys. Rev. Lett. **84**, 503 (2000).
[64] J. Kim, J. W. Wilkins, F. S. Khan, and A. Canning, Phys. Rev. B **55**, 16186 (1997).
[65] C. J. Ortiz, P. Pichler, T. Fuhner, F. Cristiano, B. Colombeau, N. E. Cowern, and A. Claverie, J. Appl. Phys. **96**, 4866 (2004).
[66] O. Boyraz and B. Jalali, Opt. Express **13**, 796–800 (2004).
[67] H. Rong, R. Jones, A. Liu, O. Cohen, D. Hak, A. Fang, and M. Pannicia, Nature **433**, 725–728 (2005).
[68] H. Rong, S. Xu, Y. H. Kuo, V. Sih, O. Cohen, O. Raday, and M. Paniccia, Nature Photonics **1**, 232 (2007).
[69] B. Jalali, V. Raghunathan, D. Dimitropoulos, and O. Boyraz, IEEE J. Sel. Top. Quantum Electron. (USA) **12**, 412 (2006).
[70] H. Rong, Y. H. Kuo, S. Xu, A. Liu, R. Jones, M. Paniccia, O. Cohen, and O. Raday, Opt. Express **14**, 6705 (2006).
[71] A. Liu, H. Rong, R. Jones, O. Cohen, D. Hak, and M. Paniccia, J. Lightwave Technol. **24**, 1440 (2006).
[72] M. A. Foster, A. C. Turner, J. E. Sharping, B. S. Schmidt, M. Lipson, and A. L. Gaeta, Nature **441**, 960–963 (2006).
[73] R. S. Jacobsen, K. N. Andersen, P. I. Borel, J. Fage-Pedersen, L. H. Frandsen, O. Hansen, M. Kristensen, A. V. Lavrinenko, G. Moulin, H. Ou, C. Peucheret, B. Zsigri, and A. Bjarklev, Nature **441**, 199–202 (2006).
[74] S. Cloutier, C. Hsu, P. Kossyrev, and J. Xu, Adv. Mater. **18**, 841–844 (2006).
[75] S. Cloutier, R. Guico, and J. Xu, Appl. Phys. Lett. **87**, 222104 (2005).
[76] M. Rafiq, Y. Tsuchiya, H. Mizuta, S. Oda, S. Uno, Z. Durrani, and W. Milne, J. Appl. Phys. **100**, 014303 (2006).
[77] S. John and S. Yang, Phys. Rev. Lett. **99**, 046801 (2007).
[78] S. Yang and S. John, Phys. Rev. B **75**, 235332 (2007).
[79] S. M. Spillane, T. J. Kippenberg, K. J. Vahala, K. W. Goh, E. Wilcut, and H. J. Kimble, Phys. Rev. A **71**, 013817 (2005).

Nonpolar Nitrides – State of the Art

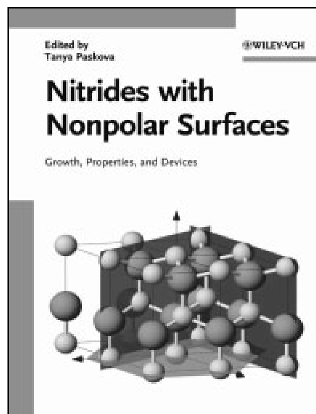

2007. Approx. 330 pages, approx. 130 figures 30 in color. Hardcover.
ISBN: 978-3-527-40768-2
Approx. € 139.- /£ 95.- /US$ 155.-

TANYA PASKOVA (Ed.)

Nitrides with Nonpolar Surfaces
Growth, Properties, and Devices

- First monograph on the state of the art of nonpolar nitrides
- Covers all nonpolar nitride materials and all known growth techniques currently under investigation
- Special emphasis on crystal growth, properties, and device studies
- Reviews the progress in heterostructures, quantum wells and dots based on the AlGaN/GaN and the InGaN/GaN systems
- Presents an outlook on application areas of materials and on capabilities and limitations of techniques
- Most renowned researchers in this field present and discuss their work

34810704_kn

Register now for the free
WILEY-VCH Newsletter!
www.wiley-vch.de/home/pas

WILEY-VCH • P.O. Box 10 11 61 • D-69451 Weinheim, Germany
Fax: +49 (0) 62 01 - 60 61 84
e-mail: service@wiley-vch.de • http://www.wiley-vch.de

© 2007 by WILEY-VCH Verlag GmbH & Co. KGaA, Weinheim